

A Synthetic Analysis of Mesoscale Precipitation System in Northeastern China Based on Satellite and Radar Data¹

Shou Yixuan^{1,2} Xu Jianmin² Shou Shaowen¹

(1. Jiangsu Meteorological Disasters Key Laboratory, Department of Atmospheric Science, Nanjing University of Information and Technology, Nanjing, 210044; 2. National Satellite Meteorological Center, Beijing, 100081)

1. Introduction

The summer rainstorms of China can be classified into the Southern, Jianghuai Meiyu, Northern Storms etc. based on geographical distribution^[1]. The rainstorms of Northeastern China possess the general features of mesoscale rainstorms. Besides, it has some special characteristics such as strong seasonality, short duration etc.^[1-2]. Affected by the unique geographical environment, the abruptness and locality are even more remarkable, which unavoidably results in considerable difficulty for weather analysis and forecasts.

Generally speaking, conventional researches on the mesoscale convective systems (hereafter is named as MCS) of rainstorms are commonly conducted via numerical prediction models or real observation data^[3], while fewer is based on the non-conventional data. Nowadays, along with the improvement of atmospheric remote sensing technology, the data such as the high-density cloud motion vector data retrieved from satellite data is one of the most effective non-conventional data. In China, a large number of high resolution satellite cloud map and its retrieved products provided by FY-2C satellite have made favorable conditions for us to reveal the dynamical characteristics of MCSs. Radar data as another supplementary data has been testified to be useful for studying some detail properties of meso- and micro-scale rainstorm systems.

In this paper, we firstly combined satellite and conventional data to investigate the relationship between the large-scale environmental field, underlying surface conditions and ground level meso-scale shear line occurred at the middle-east Heilongjiang Province after 12BST on June 10th, 2005; then further studies on the evolution process of the 3-D kinetic structure characteristics of the MCS on the upper reach of Shalan River are performed by radar and satellite data to advance recognition of rainstorms MCS.

2. Data and Methods

Data used in this article are as follows:

- Observational data: sounding record; 24 hour precipitation record and $1^{\circ} \times 1^{\circ}$ NCEP reanalysis data in once every 6 hours.
- FY-2C geo-synchronous satellite data: include the cloud map data in once an hour (0500 UTC ~ 0600 UTC are spaced half an hour apart); the $1^{\circ} \times 1^{\circ}$ cloud motion vector data in once every 6 hours; $0.1^{\circ} \times 0.1^{\circ}$ TBB data in once an hour; $0.1^{\circ} \times 0.1^{\circ}$ once a hour ground incoming solar radiation data.
- Doppler radar record: the data about once every 6 minutes obtained by model 3830 C-band weather radar in Mudanjiang city under the operation mode of stereo-scanning (VCP 21).
- GIS data: Digital Elevation Model (DEM) data with spatial resolution: $0.00833^{\circ} \times 0.00833^{\circ}$.

In this article, for the demand of analyses, we converts and displays the radar reflectivity intensity (Z) on the iso- elevation angle surface under polar coordinate to the constant altitude plane under the Cartesian coordinate system. The ellipsoid Cressman interpolating function^[4] is

¹ This work is supported by Chinese NNSF(40405009,40575022,40205008); Jiangsu Weater Bureau Program (200406) ; Jiangsu Meteorological Disasters Key Laboratory program KLME050201, Jiangsu Natural Science Foundation (BK2005141)

used here for interpolation. The scope of horizontal interpolation is (44.1 °N-44.75 °N) (128.45 °E-129.25°E), grid spacing is 0.01°×0.01 °. The vertical range is from 1.5 to 12.5 km with 0.5 km grid spacing. The horizontal and vertical action radii of the interpolating function are assumed to be 2.5 km and 1.5 km respectively.

The adopted wind field retrieval method herein is the U-W (Uniformed Wind) inversion technique [5]. According to the given condition of the U-W method we precede wind field reversion with the radial wind speed upon low elevation angle layer of radar data and make an iso- elevation interpolation with ellipsoid Cressman interpolation function. The horizontal grid spacing is assumed to be 0.01°× 0.01°. Since the mid-lower layer wind fields are closely related to the occurrence and development of MCS, this article is focused on the study of wind field distribution whose vertical range is 1.5-5.5 km with 0.5km grid spacing. A smoothing filtering on the retrieved horizontal wind field is performed to wipe off some useless micro-scale information. The unmeasured points within the record are not involved in the smoothing process of the wind field.

3. Weather Facts and Upper Air Circulation Situation

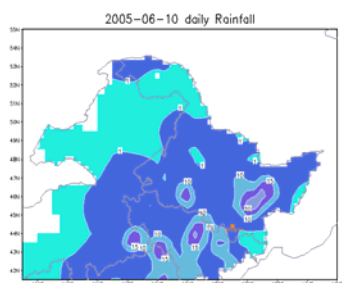


Fig.1 daily rainfall distribution reached 35.6mm at 14BST.

With respect to the largescale condition, the upper-air circulation has taken on a two ridges and one trough pattern with two blocking highs near the Ural Mountain and Yakutsk area and a broad and stable long wave trough region lies on the Baikal Lake area since 20 BST, June 9th 2005. This pattern was relatively stable until 08BST June 10th. From that time the Ural high was enhanced and extended eastward and combined with the Yakutsk high on the east. The northwest air stream was intensified substantially. This time the stormy region was located before the upper air trough.

Fig. 1 is the daily rainfall map observed by rain-gauge station between 08BST June 10th-11th, 2005. It can be seen from the figure that there is a rainfall ribbon extending from southwest to northeast over the mid-east region of Heilongjian and Jilin Provinces of China. According to the precipitation retrieved by radar data, the severe precipitation at upper branch of Shalan River seems occurred around 12BST and ended at 15 BST, totally lasting 3 hours. During the process, the maximum 1h precipitation

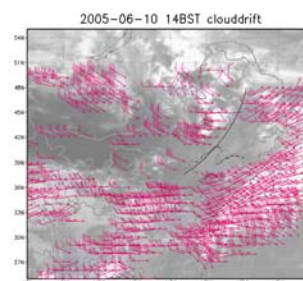


Fig 2 Upper level (100hPa-400hPa) cloud motion vector maps (Unit: m/s)

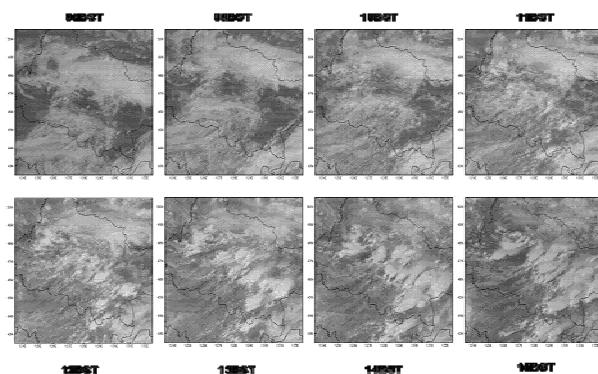


Fig.3 Visible cloud images of FY-2C geosynchronous satellite from 08BST to 15BST June 10th, 2005

Fig.2 is the superposition of IR cloud images and upper level cloud motion vector maps during the rainstorm. It can be seen that there is a comma cloud mass over the stormy region corresponded by an obviously divergence and an anti-cyclonic inflection in the upper-level cloud motion vectors field. In addition, there was a piece of thinner and lower stratified cloud lying in front of the trough line during the whole process which is obscured seen on the IR channel images but clearly on the visible cloud map(Fig. 3).

From 11BST, along the rim of this stratified cloud area a series of convective cloud masses are stimulated and moved northeastward. In a word, the rainstorm is occurred in the process of the upper-level trough moving eastward and deepening and the diverging-converging mechanism between upper and lower level acts as the important large-scale dynamic factor for this case.

4. Upper/Lower-Air Thermodynamic Energy Distribution and Stability Analysis

Fig. 4 presents the variation of the wind direction against the latitude at one sounding station which located in front of the upper trough before rainstorm was occurred. The fact that wind direction of lower (upper) troposphere in front of the upper trough apparently shift clockwise (counterclockwise) against altitude indicates the lower (upper) level of troposphere was warm advection (cold advection) over the trough front region of the upper trough.

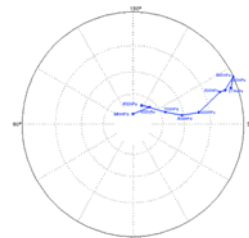


Fig.4 Wind directions over Haerbin

Fig. 5 is the 850 hPa θ_{se} distribution graph of 08BST of June 10th, 2005. It can be seen from the chart that there is a moist tongue extending from southwest to northeast, stretching from the mid-east Liaoning, Jilin Province to the mid-east part of Heilongjiang Province. The iso-specific humidity lines are very dense on the northwest of the moist tongue. Along with this moist tongue, the southwest wind on the lower level transport the water vapor to the vicinity of rainstorm area, which provided favorable water vapor condition to strong precipitation. On the cross-section the range of moist tongue was about from 125.5 ° -130.5 °E. The EW sides of the moist tongue within mid-lower parts of troposphere are low-value regions. Over the moist tongue, the lower (mid-upper) level of troposphere is the region with high (low) θ_{se} , thus resulting the stratification in an instability. Coincided with the temperature differential advection, humidity differential within the precipitation area is another significant factor for the rainstorm.

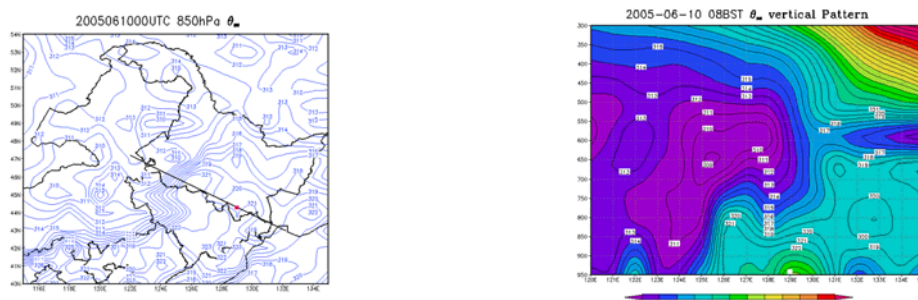


Fig.5 a) 850hPa θ_{se} (Unit: °K) at 08BST on June 10th 2005 ; b) θ_{se} cross-section along the thick solid line in fig. 5a

However, according to the TT index ^[6] map over the precipitation area it seems that strong convections did not occur in all areas with high TT index, nor does the highest TT index correspond to the strongest convection. Question about such phenomenon is reasonably raised. To give answers to such a question, it is useful to begin from the analysis of the moisture-temperature condition at the underlying surface of that time.

Based on the weekly accumulated precipitation map of Northeast China before June 10th, it is seen that there is a NE-SW rain band lies in the midst of Heilongjian Province during the week. The continuous rainfall made underlying surface of the stormy region rather wet. Compared to the visible cloud images (Fig.3) and 850 hPa θ_{se} distribution graph (Fig.5), we found that the trend and position of that thinner and lower stratified cloud area was roughly agree with that of the lower level moist tongue even the rain band on the weekly rain map. Since the upper air of the

moist tongue was covered by clouds, the solar radiation received by ground was relatively low. That is to say the ground was unevenly heated by the incoming solar radiation. This kind of uneven heating has been quantitatively verified by the incoming solar radiation product of FY-2 meteorological satellite (Fig.6). From the figure we can see that, starting from 11BST, a series of convective cloud mass are occurred along that non-coherent solar energy boundary (colored by yellow) which demonstrates that the non-uniform heating of underlying surface is the thermodynamic trigger mechanism of strong convection.

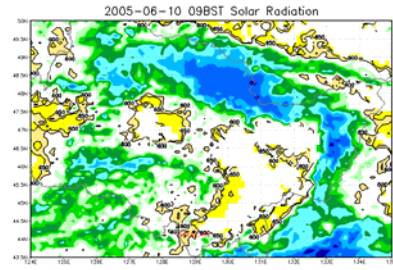


Fig.6 Solar energy received by underlying surface at 09BST June 10th, 2005 (Unit:W/m²)

Moreover, the development of a ground meso-scale shear line is considered as another factor for the phenomenon on the TT index map. Compositing the shear line and the cloud image (as shown if Fig.7), it is obviously seen that not only the position and shape of this ground shear line coincide with the line of energy discontinuity on the incoming solar radiation energy distribution map but also the distribution of convective cloud clusters was almost identical with the trend of shear line. And the distribution of overshooting interior of the convective cloud masses seems also has closed relationship with this shear line (most of them are seen to be centralized at tail of convective cloud mass near the shear line and the highly dense area of the overshooting is roughly located at the maximum curvature of the shear curve).

Fig.7 The composite map of the 925hPa moisture field, surface winds, and FY2C visible image at 14BST, June 10th, 2005 (isolines denote specific humidity line; thick solid line denote the surface mesoscale shear line; 'C' is the surface cyclone center; the little circles are the location of the overshooting cloud tops)

As Dr. J.F.W Purdom once indicated that (individual discussion), on the sector where the shear line are approximately parallel with the ambient airflow, the convection cell of downstream was involved into the humid air flow horizontally from the upper stream, which makes the convection easier to develop. Thus, with the south-west flow, such kind of mechanism will result in the augment of water vapor within the mid-high layer of troposphere, thickening of the humid layer and further promoting the development of convection at the maximum curvature point.

5. The dynamic structural feature and evolutionary process of MCS

As for the dynamic structure and evolutionary process of MCS, we will stress to investigate some details features of the MCS over Shalan River region. According to the rainfall amount, the investigation is segmented into three phases: the firstborn stage, development and the stage of ripeness.

5.1 The firstborn stage of MCS

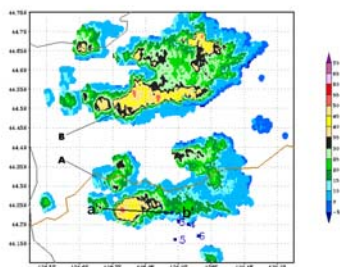


Fig.8a Echoes at 3km (Unit: dbz)

From the time series evolution of radar echo at this phase, the strong echoes above 40 dbz in cloud cluster 'A', which was seen to be just over Shalan River area during the rainstorm, were concentrated locally at the southwest rear of the cloud cluster. During the course when it moved from southwest to northeast, curling phenomena appeared on both ends of it. At 11:48BST, there appears an apparent velocity convergence in the 1.5km horizontal wind field within the strong echo area of cloud cluster A. To the east of the

convergence area the airflow presents a fanshaped disperse structure. A weak anti-cyclonic circulation with ~10 km horizontal scale was adjacent to the strong echo area. In the vertical direction (Fig 8b), the airflow ascend from the west and sink on the east. Although ordered ascending and descending movement has been formed within the cloud body, compared with the sinking airflow, the rising airflow is relatively weaker in this stage.

5.2 Stage of Development

During this stage, the radar echo got more intense and the

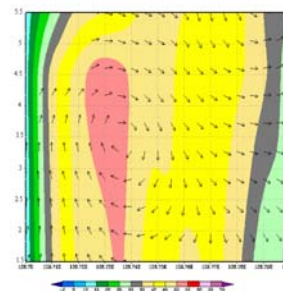


Fig. 8b Composite map of echoes and u-w wind fields Cross-section in WE direction

areas above 50 dbz moved closer to the range of upper branch of Shalan River. The vertical cross-section along the S.W.-N.E. direction crossing the strongest echo area shows that the strong echo above 60 dbz appeared at the middle layer of convective cloud cluster 'A' while the top of 50 dbz strong echo approached 8 km. The zone of convergence was still located on the brim on the western side of cloud mass 'A'. At this point, except for the southwesterly and westerly winds, easterlies emerged in the vicinity of the zone of convergence. Compared with the last stage, the anti-cyclonic rotational dispersing becomes more evident. Yet as the altitude increases, this feature becomes more and more unobvious. Furthermore, the position of the sinking area happens to correspond with the anti-cyclonic circulation of lower elevation. Since the rainfall substance will evaporate and cool during the procedure of falling. When the sinking airflow in the cloud rushed to the vicinity of ground, these kinds of cold and almost saturated airflow will disperse to the circumference making a meso-scale surface high-pressure area. That is to say, the anti-cyclonic circulation stimulated on the west side of low altitude wind field might be the manifest of meso-scale high pressure triggered by ground rainfall upon the wind field.

5.3 Stage of Ripeness

It can be inferred from the wind field distribution that the major characteristics of low altitude wind field at this phase is the enlarging of horizon scale and the strengthening of the intensity of the meso-scale thunderstorm high. Compared with the previous phases, the anti-cyclonic circulation within the strong echo area was further enlarged and deepened even becoming completely closed (Fig.9). On the cross-section map, the divergence airflow converges with the incoming airflow and brought about a more intensive ascending motion. This shows that this cyclonic circulation represent the intensification of thunderstorm high at this phase.

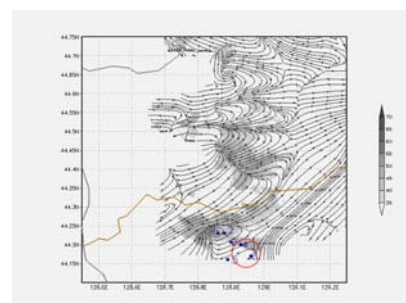


Fig. 9 Stream fields at 1.5km

6. Conclusion and Discussion

This article applied the method of incorporating routine meteorological observation, satellite and radar data thoroughly studied the large scale condition and meso-scale shear line and the 3D kinetic structure and evolutionary characteristics of the MCSs occurred in the middle-east part of Heilongjiang Province during the afternoon of June 10th, 2005. The result of analysis indicated that:

1) This rainstorm is a convective weather procedure occurred as the high altitude shortwave trough moved eastward and deepened. The meso-scale convective system lay in front of the forward leaning and scattered upper trough. The divergence mechanism provided favorable large

scale dynamic condition for the occurrence of MCS.

2) A SW-NE moist tongue at the lower level of troposphere provided favorable water vapor condition for the rainstorm; in addition, the differential advection formed by the temperature and moisture advection between upper and lower level enhanced the instability of stratification of the atmosphere at this point.

3) Circulation aroused by the non-uniform heating owing to the difference of solar radiation is considered as the thermodynamic trigger of MCS during this procedure of rainstorm; and the evolution of an underlying meso-scale shear line have close relationship with the occurrence and development of this rainstorm convective system.

5) By synthesizing the features of generation, evolution and maturation phases of the MCS of this case of rainstorm, the MCS resulted in heavy rain over upstream of Shalan River of Heilongjiang Province on June 10th, 2005 was an isolated convection system with the structural feature of multi-cell storm.

6) As respect to the dynamical structure properties, the low altitude wind fields of the three phases presented apparent regularity. Anti-cyclonic airflows at low level within the rain area are gradually strengthened and systematically organized with the development of the rainfall.

7) For the entire convective cloud, treat the migrating direction (northeast) of the cloud mass as the front, the warm and humid air at lower altitude flew in from left-rearward (southwest) of the cloud cluster and generates ascending motion while flew out on the right front (northeast). This is opposite to the feature of Northeastern China rainstorm analyzed in this article.

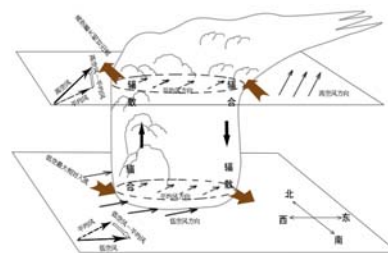


Fig.10 Schematic of the left moving storm

8) As for the kinetic characteristic of the storm, it acts as a left moving storm^[7]. According to the schematic diagram of this storm (Fig. 10), treating the mean wind (southwesterly) direction of cloud layer as front, the left (right) side airflows converge (diverge) at lower level and diverge (converge) at upper. It is such inhomogeneous distribution of divergence in horizontal and vertical that causes the MCS to act as a left moving storm.

Reference

- [1] Tao Shiyun. Chinese Rainstorm. Beijing: Science Press. 1980:115
- [2] Zhen Xiuya, Zhang Tingzhi, Bai Renhai. Rainstorm in Northeastern China. Beijing: China Meteorological Press.1992:1-19
- [3] Sun Li, An Gang. A Diagnostic Study of Northeast Cold Vortex Heavy Rain over The Songhuajiang-Nenjiang River Basin in the Summer of 1998.Chinese Journal of Atmospheric Sciences(in Chinese), 2001,25(3):342-354
- [4] Zhou Haiguang, Zhang Peiyuan. A new technique of recovering Three-Dimensional wind fields from simulated dual-Doppler radar data in the Cartesian space. Acta Meteorologica Sinica(in Chinese). 2002,60(5):585~593
- [5] Wang Fengyun, Wang Yanxiong, Tao Zuyu. The study of mesoscale wind field detection technique for single doppler weather radar. Journal of Tropical Meteorology (in Chinese), 2003,19(3):291-298
- [6] Shou Shaowen, Li Shenshen, Yao Xiuping. Mesoscale Meteorology. Beijing: China Meteorological Press. 2003: 285-291; 295-296.
- [7] Schmid, W. et al., 1990: Severe left-moving hailstorms in central Switzerland. Preprints, 16th Conference on Severe Local Storms, Kananaskis Provincial Park, Alberta, 467-472.